New AC Resistance Calculation of Printed Spiral Coils for Wireless Power Transfer

Gaorong Qian, Yuhua Cheng*, Guoxiong Chen, Gaofeng Wang
Hangzhou Dianzi University, Hangzhou, China
*E-mail: chengyh@hdu.edu.cn

Abstract

Wireless power transfer (WPT) is a promising technique for powering the Internet-of-Things devices. Printed spiral coils (PSCs) are commonly used in WPT because of their advantages of compact size and standardized fabrication. Under the demand of analytically optimizing the WPT system, like power transfer efficiency or power delivered to the load, an analytical resistance model is required. In this paper, the proximity-effect resistance is focused on. A formula is curve-fitted based on the data simulated from COMSOL Multiphysics and magnetic field calculation. The total AC resistance model which is the sum of skin-effect resistance and proximity-effect resistance is verified by HFSS simulation and measurement. Under the impact of inductance and parasitic capacitance, the comparison of the calculated, simulated, and measured real parts of *Z*-impedance shows that the difference between them is increased quickly when the operating frequency is higher than the frequency corresponding to the maximal quality factor of a PSC. A more accurate self-resonant frequency or capacitance model should be developed in the future work.

Keywords

Resistance, printed spiral coil, wireless power transfer

1. Introduction

The vision of the Internet-of-Things (IoT) projects deployment of a large number of devices everywhere. One of the significant challenges for this vision is powering all the devices cost-effectively and conveniently. Instead of replacing the battery of IoT devices, harvesting energy from ambient energy sources [1] or receiving power from dedicated power transmission sources (i.e., wireless power transfer, WPT) [2] [3] are promising techniques and draw amount of attention recently.

Printed spiral coils (PSCs) are commonly used in inductively coupled wireless power transfer (ICWPT) and other applications like near field communication, and radio frequency identification, by virtue of compact size, standardized fabrication, and good uniformity for PSCs [4]. In ICWPT, the power transfer efficiency, one of the most important parameters concerned, is determined by the coupling coefficient and the quality factors of the coupled coils, which are related to the geometries of the coils. A fully analytical model of the coils are required to optimize the geometries of the coils to reduce the power loss and improve the efficiency. The modelling of the self- and mutual inductances have been established analytically and accurately. Although many efforts have been exerted on studying the AC resistance of PSC [5], an accurate model is still absent. Two mechanisms induce the increase of the resistance with frequency, i.e., skin-effect and proximity-effect. The skin-effect resistance has been studied and an accurate model has been obtained [7], [8]. In this paper, the proximity-effect resistance is analytically modelled. The resistance model is verified by simulation and experiments within the frequency range of lower than the self-resonant frequency of a PSC.

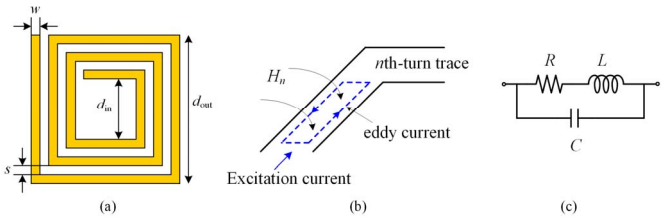

Figure 1: (a) Diagram of multi-turn PSC, (b) proximity effect and eddy current, and (c) lumped resistance, inductance, and capacitance model

2. proximity-effect resistance

A *N*-turn PSC is shown in Fig. 1a where the outer and inner diameters are d_{out} and d_{in}, respectively, the space between the adjacent trace is *s*, the thickness and width of the trace are *t* and *w*, respectively. If an AC current is fed into the conductor, the current will crowd to the edges of the conductor, which is the phenomenon named skin-effect and leads to the increase of the resistance. Another current crowding phenomenon is caused by the proximity effect as shown in Fig. 1b where a top view of the eddy current in the n^{th} turn, induced by a magnetic field from the current of other conductors. This eddy current results in asymmetrical current distribution between two sides of a conductor and consequently the increase of the resistance furthermore. In previous studies, authors considered the eddy currents to be simply limited in the outer 1/4 of the trace width [9], [10] or δ of the trace width [11], where δ is the skin-depth. This simplification give a rough approximation of resistance. Although electromagnetic simulation tools and some finite element method [12] can give more accurate results, the accuracy is dependent on the number of elements and usually it is time consuming.

Based on the analytical calculation method of the proximity-effect resistance (R_{pr}) for a conductor with circular cross-section [13], a similar method is proposed [4],

$$R_{pr} = \sum_{1}^{N} R_{pr,n} = \sum_{1}^{N} \left(l_n \cdot \frac{4\pi}{\sigma} \cdot \Phi \cdot H_n^{\,2} \right), \qquad (1)$$

where $R_{pr,n}$ is the proximity-effect of the n^{th} turn, l_n is the trace length of the n^{th} turn, σ is the conductivity of the copper, H_n is the magnetic field normal to the conductor surface when the excited current is 1 A, and Φ is a function

of w, t, and δ, $\delta = (\pi\mu_0\sigma f)^{-0.5}$ where μ_0 and f are the permeability of the copper and the operating frequency. Although the simulated values of $\Phi(w/\delta, t/\delta)$ are plotted in [4], a formula is required to express the resistance and consequently the quality factor and efficiency in optimizing WPT analytically. Fig. 2 shows an example of the eddy current distribution simulated in COMSOL Multiphysics where 1-A/m magnetic field in the vertical direction is added to the conductor and no external current is excited. The power loss of an unit-length copper conductor can be calculated according to the simulation, consequently the values of Φ is extracted according to (1). Based on 10000 cases with the trace width range from 0.1 mm to 10.333 mm (50 points), the operating frequency range from 0.1 MHz to 1.6 GHz (200 points), a curve-fitted formula is obtained

$$\Phi = -0.998 + 0.112\frac{w}{t} - 0.689\frac{t}{\delta} + 0.543\frac{w}{\delta} + 0.002\left(\frac{w}{t}\right)^2. \quad (2)$$

The magnetic field normal to the surface of the n^{th} turn, i.e., H_n, in (1) can be calculated by summing all the magnetic field produced by the currents inside other turns [11], [14], [15]. A more concise method is approximated as [9]

$$H_n = \frac{0.22}{w+s}\frac{4n-N}{N}. \quad (3)$$

3. Verification by simulation and measurement

In order to verify the modeling of the proximity-effect resistance, simulation and measurement are taken. The difficulty of verification is from the truth that the resistance of the PSC is not independent from the impedance, i.e., only the impedance of the PSC but not the resistance can be obtained from simulation tools or measurement devices. If a multi-turn PSC is modelled by an inductor L and a parasitic resistance R in series, and a parasitic capacitance C in parallel (as shown in Fig. 1a), the real and imaginary parts of the Z-impedance of PSC coil can be expressed as

$$\begin{aligned}\mathrm{Re}(Z) &= \frac{R}{\left(1-\omega^2 LC\right)^2 + \left(R\omega C\right)^2} \\ \mathrm{Im}(Z) &= \frac{\left(1-\omega^2 LC\right)\omega L - R^2\omega C}{\left(1-\omega^2 LC\right)^2 + \left(R\omega C\right)^2}\end{aligned}, \quad (4)$$

where ω is the angular frequency, $\omega = 2\pi f$. The lumped inductance and capacitance have a self-resonant frequency ($f_{\text{sr}} = 1/(2\pi(LC)^{0.5})$ which impacts on Z-impedance. When $f << f_{\text{sr}}$, Re(Z) can be simplified to R. When f is high, especially when f is close to f_{sr}, Re(Z) is much larger than R, and increases with f faster than the situation when f is low. That is to say, an accurate self-resonant frequency or parasitic capacitance model is important to verify Re(Z) besides an accurate inductance model, if the operating frequency range up to the self-resonant frequency should be considered. Although a good inductance model [16], as shown in (6), exists, to the best of our knowledge, an accurate model of self-resonant frequency or parasitic capacitance still is absent now. Here, a simple model with moderate accuracy of self-resonant frequency in [17] is

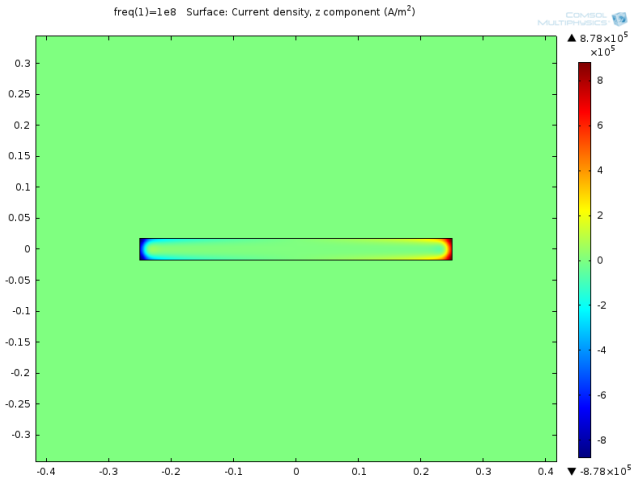

Figure 2: Eddy current distribution of a conductor under a magnetic field normal to its surface

selected here,

$$f_{\text{sr}} = \frac{0.2615c}{l}, \quad (5)$$

where c is the velocity of electromagnetic wave, and l is the total length of the conductor. Then the parasitic capacitance can be obtained from f_{sr} and L,

$$\begin{aligned}L &= 0.635\mu_0 d_{\text{avg}} N^2\left[\ln\left(2.07/\rho\right) + 0.18\rho + 0.13\rho^2\right] \\ C &= \frac{1}{\left(2\pi f_{\text{sr}}\right)^2 L}\end{aligned}, \quad (6)$$

where $d_{\text{avg}} = (d_{\text{out}}+d_{\text{in}})/2$, $\rho = (d_{\text{out}} - d_{\text{in}})/(d_{\text{out}} + d_{\text{in}})$.

In (4), R is the total resistance, i.e., the sum of skin-effect resistance R_{sk} and R_{pr}. R_{sk} can be found from [7],

$$\begin{aligned}R_{\text{sk}} &= \frac{l}{\sigma w t}\left[1 + \left(f/f_1\right)^2 + \left(f/f_0\right)^5\right]^{0.1} \\ f_1 &= \frac{\pi}{2\mu\sigma w' t'} \\ f_0 &= \frac{\pi^2}{\mu\sigma w' t'}\left[K\left(\sqrt{w'^2 - t'^2}/w'\right)\right]^{-2}\end{aligned}, \quad (7)$$

where $K(\cdot)$ is the complete elliptic integral of the first kind, $w' = w/(\pi)^{0.5}$, and $t' = t/(\pi)^{0.5}$, respectively.

With the preparation of (4)–(7), a set of PSCs are fabricated, simulated, and measured, which are with various trace widths and spaces. All other geometrical parameters are fixed as follows: t = 35 μm, N = 11, and $d_{\text{out}} = w + 70$ mm. The trace width w varies from 0.5 mm to 2.1 mm with step 0.4 mm, while the trace space s is set in such a way that $(w + s)$ is always equal to 2.5 mm.

Fig. 3 shows the measurement setup where the coil is connected to a vector network analyzer (VNA Agilent E5071C) through a SMA connector, the parasitic parameters of which is removed partly by using de-embedding method [18]. The simulation is completed in Ansoft HFSS.

Table I shows the measured, simulated, and calculated self-resonant frequencies for different cases. Because of the impact of the environment and the substrate of the PSC, i.e.,

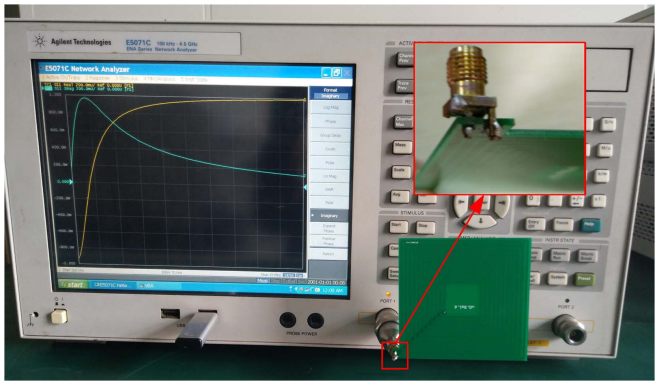

Figure 3: Measurement setup by using a VNA

Table 1: Measured, simulated, and calculated self-resonant frequencies under different trace width cases.

Trace width (mm)	0.5	0.9	1.3	1.7	2.1
Mea. f_{sr} (MHz)	30.1	29.5	29.0	27.0	27.0
Sim. f_{sr} (MHz)	53.0	48.0	47.0	46.0	45.0
Calc. f_{sr} (MHz)	39.6	39.6	39.6	39.6	39.6

FR4 material with 4.4 permittivity, the parasitic capacitance in practice is larger than the simulated and calculated ones. Consequently, the measured self-resonant frequency is lower than the simulated and calculated ones. As a fair comparison and removing the influence of the difference of self-resonant frequencies between measured, simulated, and calculated results, in calculation, different self-resonant frequency is set in the following comparison.

Fig. 4a–4c shows the comparison between the calculated, simulated, and measured Re(Z) for the cases of w = 0.5 mm, 1.3 mm, and 2.1 mm, respectively. We can observe from Fig. 4, when f is lower than 10 MHz, the measured, simulated, and calculated Re(Z) which equal to R approximately, are close to each other. We also find that the error increases with w, i.e., the error for case w = 2.1 mm is larger than the case w = 0.5 mm. The reason is the approximated calculation of magnetic field in (3) with larger error when the trace width is larger. When f is higher than 10 MHz, the impact of the self-resonant frequency increases. In calculation, when the self-resonant frequency is adjusted to the values same with simulated or measured self-resonant frequency, the calculated Re(Z) are also with acceptable accuracy.

In the application of WPT, the optimal operating frequency, corresponding to the maximal power transfer efficiency, is usually chosen to be the frequency where the quality factors of PSCs are maximized [19]. According to the measured quality factors for the cases, shown in Fig. 5, where the frequencies corresponding to the maximal quality factors are about 10 MHz which is the boundary if the impact of the self-resonant frequency becomes obvious or not.

4. Conclusion and future work

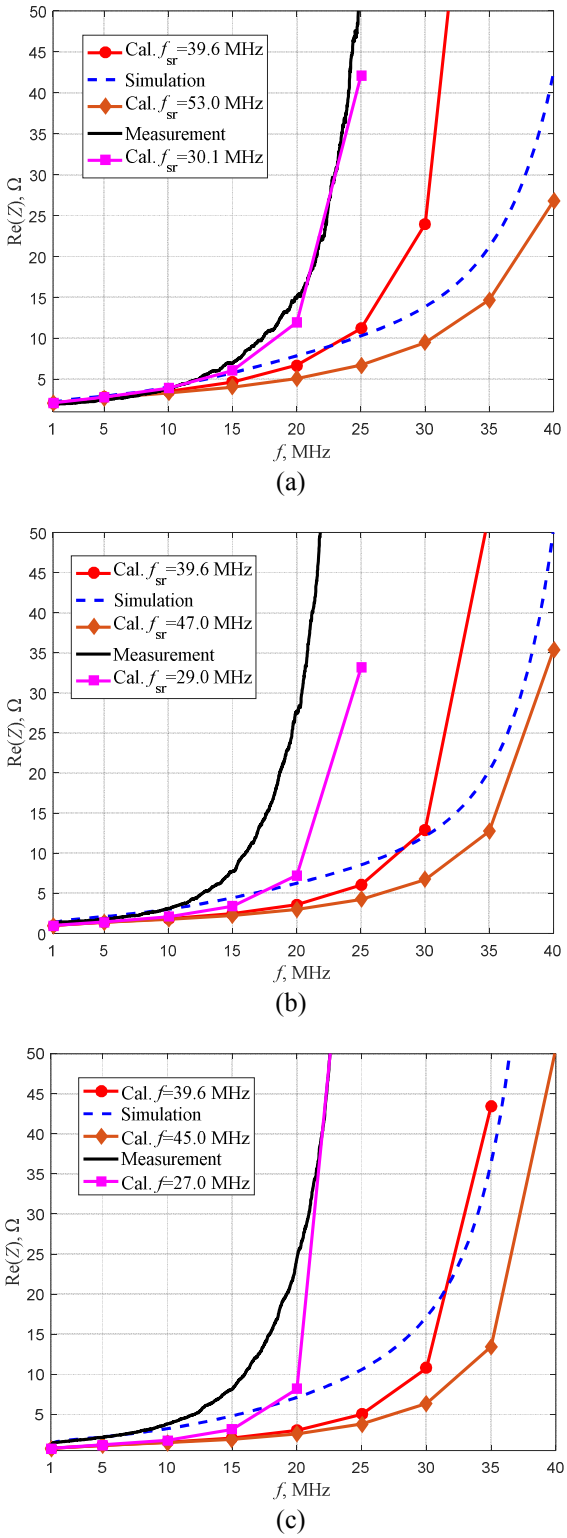

Figure 4: Comparison between the calculated, simulated, and measured Re(Z) for different cases, (a) w = 0.5 mm, (b) w = 1.3 mm, and (c) w = 2.1 mm, respectively.

A simple and accurate formula of proximity-effect resistance for PSCs is developed by curve-fitting the resistance of unit-length conductors with rectangular cross-section under unit magnetic field normal to the surface and calculating the magnetic field distribution for multi-turn

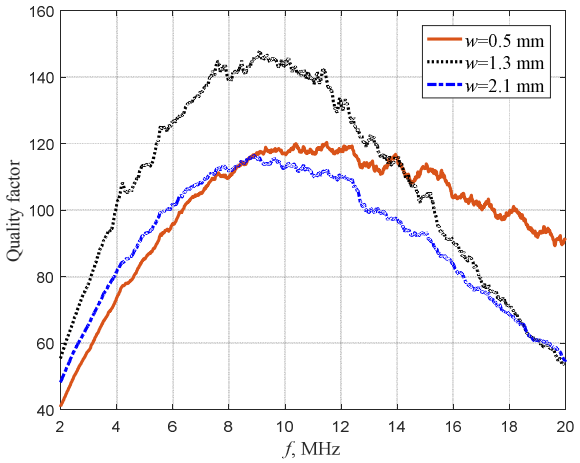

Figure 5: Measured quality factor for different cases.

PSCs. The simulated and measured results show that the model has good accuracy. When the operating frequency is high, the impact of self-resonant frequency leads to the difference between the calculated, simulated, and measured real parts of *Z*-impedance increase. The frequency boundary of this impact becoming obvious or not is the same with the frequency corresponding to the maximal quality factor. In the future work, an accurate model of parasitic capacitance or self-resonant frequency is required to obtain a more accurate PSC analytical model.

5. Acknowledgement

This work was supported by the Zhejiang Provincial Natural Science Foundation of China under grant No. LY17F010018 and the Natural Science Foundation of China under grants No. 61411136003 and No. 61771175.

6. References

[1] M. A. Abouzied, K. Ravichandran, and E. Sánchez-Sinencio, "A Fully integrated reconfigurable self-startup RF energy-harvesting system with storage capability", IEEE J. Solid-State Circuits, 2017, 52(3), pp. 704–719.

[2] Y. Cheng and Y. Shu, "A New Analytical Calculation of the Mutual Inductance of the Coaxial Spiral Rectangular Coils," IEEE Trans. Mag., 2014, 50(4), No. 7026806.

[3] P. Yang, L. Dong, Y. Jing, et al., "A study of wireless power transfer for implantable devices by using wearable devices," IEEE 16th International Conference on Communication Technology, pp. 626–629, 2015.

[4] I. Lope, C. Carretero, J. Acero, et al., "AC power losses model for planar windings with rectangular cross-sectional conductors", IEEE Trans. Power Electron., 2014, 29(1), pp. 23–28.

[5] U. M. Jow and M. Ghovanloo, "Design and optimization of printed spiral coils for efficient transcutaneous inductive power transmission", IEEE Trans. Biomed. Circ. Systems, 2007, 1(3), pp. 193–202.

[6] D. H. Kim and Y. J. Park, "Formula of parallel straight planar conductors for minimum ohmic resistance", Electron. Lett., 2016, 53(2), pp. 121–123.

[7] A. W. Lotfi and F. C. Lee, "Two-dimensional skin effect in power foils for high-frequency applications", IEEE Trans. Mag., 1995, 31(2), pp. 1003–1006.

[8] C. Patrick Yue and S. Simon Wong, "Physical modeling of spiral inductors on silicon," IEEE Trans. Electron Devices, 2000, 47(3), pp. 560–568.

[9] W. B. Kuhn and N. M. Ibrahim, "Analysis of current crowding effects in multiturn spiral inductors", IEEE Trans. Microw. Theory Tech., 2001, 49, (1), pp. 31–38.

[10] C. Wang, H. Liao, C. Li, et.al., "A wideband predictive "double□π" equivalent□circuit model for on□chip spiral inductors", IEEE Trans. Electron Devices, 2009, 56(4), p. 609–619.

[11] K. Y. Tong and C. Tsui, "A physical analytical model of multilayer on□chip inductors", IEEE Trans. Microw. Theory Tech., 2005, 53(4), p. 1143–1149.

[12] D. H. Kim, and Y. J. Park, "Calculation of the inductance and AC resistance of planar rectangular coils", Electron. Lett., 2016, 52(15), p. 1321–1323.

[13] J. A. Ferreira, "Improved analytical modeling of conductive losses in magnetic components", IEEE Trans. Power Electron., 1994, 9(1), pp. 127–131.

[14] J. M. Lopez-Villegas, J. Samitier, C. Cané, et al., "Improvement of the quality factor of RF integrated inductors by layout optimization", IEEE Trans. Microw. Theory Tech., 2000, 48(1), pp. 76–83.

[15] N. M. Ibrahim and W. B. Kuhn, "An approach for the calculation of magnetic field within square spiral inductors at low frequency", Intern. J. Numer. Modell.: Electronic Networks, Devices and Fields, 2002, 15(4), pp. 339–354.

[16] S. S. Mohan, M. del Mar Hershenson, S. P. Boyd, et al., "Simple accurate expressions for planar spiral inductances", IEEE J. Solid-State Circuits, 1999, 34(10), pp. 1419–1424.

[17] N. Maleeva, M. V. Fistul, A. Karpov, et al., "Electrodynamics of a ring-shaped spiral resonator", J. Applied Physics, 2014, 115, No. 064910.

[18] Y. Cheng, G. Wang, and M. Ghovanloo, "Analytical modeling and optimization of small solenoid coils for mm-sized biomedical implants", IEEE Trans. Microw. Theory Techn., 2017, 65(3), pp. 1024–1035.

[19] Y. Cheng, D. Xuan, X. Su, et al., "An optimal operating frequency selection scheme for maximizing inductive power link efficiency", Microw. Opt. Techn. Lett., 2018, in press, No. MOP31016.